JOURNAL OF VIROLOGY, Mar. 1997, p. 2331–2341 Vol. 71, No. 3
0022-538X/97/$04.00+0

Assembly of African Swine Fever Virus: Role of Polyprotein pp220

GERMÁN ANDRÉS, CARMEN SIMÓN-MATEO,† AND ELADIO VIÑUELA*

Centro de Biología Molecular "Severo Ochoa" (Consejo Superior de Investigaciones Científicas-Universidad Autónoma de Madrid), Universidad Autónoma de Madrid, Cantoblanco, 28049 Madrid, Spain

Received 8 November 1996/Accepted 6 December 1996

Polyprotein processing is a common strategy of gene expression in many positive-strand RNA viruses and retroviruses but not in DNA viruses. African swine fever virus (ASFV) is an exception because it encodes a polyprotein, named pp220, to produce several major components of the virus particle, proteins p150, p37, p34, and p14. In this study, we analyzed the assembly pathway of ASFV and the contribution of the polyprotein products to the virus structure. Electron microscopic studies revealed that virions assemble from membranous structures present in the viral factories. Viral membranes became polyhedral immature virions after capsid formation on their convex surface. Beneath the lipid envelope, two distinct domains appeared to assemble consecutively: first a thick protein layer that we refer to as core shell and then an electron-dense nucleoid, which was identified as the DNA-containing domain. Immunofluorescence studies showed that polyprotein pp220 is localized in the viral factories. At the electron microscopic level, antibodies to pp220 labeled all identifiable forms of the virus from the precursor viral membranes onward, thus indicating an early role of the polyprotein pp220 in ASFV assembly. The subviral localization of the polyprotein products, examined on purified virions, was found to be the core shell. In addition, quantitative studies showed that the polyprotein products are present in equimolar amounts in the virus particle and account for about one-fourth of its total protein content. Taken together, these results suggest that polyprotein pp220 may function as an internal protein scaffold which would mediate the interaction between the nucleoid and the outer layers similarly to the matrix proteins of other viruses.

African swine fever virus (ASFV), the causative agent of a highly lethal disease of domestic pigs, is one of the most complex animal viruses (10, 38). Its genome structure, a double-stranded linear DNA molecule with covalently linked ends and terminal inverted repetitions, is similar to that of poxviruses (16, 35). However, the virus particle shows a morphology very similar to that of iridoviruses (8). Currently, ASFV is the only member of the African swine fever-like virus genus (12). The virus particle, composed by more than 30 different polypeptides (7, 15), possesses a complex structure constituted by several concentric domains with an overall icosahedral shape and an average diameter of 200 nm. According to the current model, the inner component is a DNA-containing nucleoid which is enwrapped by a lipid envelope and an icosahedral capsid (8). Extracellular virions usually possess an additional lipid envelope acquired by budding from the plasma membrane (4).

The ASFV genome, which ranges between 170 and 190 kbp, depending on the virus strain, has been recently sequenced in our laboratory for the avirulent isolate BA71V, and about 150 potential genes have been identified (39). One of the most striking features of ASFV gene expression is the synthesis of polyproteins to produce some of the major components of the virus particle. The structural proteins p150, p37, p34, and p14 are produced after posttranslational processing of an N-myristoylated polyprotein precursor, named pp220, which is synthesized after DNA replication (1, 33). In addition, we have recently shown that the structural proteins p35 and p15 derive from a 62-kDa polyprotein precursor (32). This strategy of gene expression, unusual in DNA-containing viruses, is common in positive-strand RNA viruses and retroviruses (19, 20). In these cases, proteolytic processing of structural polyproteins is usually related to the viral morphogenesis determining the coordinated assembly of the mature products that form the virus structure.

Very little is known about ASFV assembly. Early works showed that virus particles assemble in discrete cytoplasmic areas close to the nucleus referred to as viral factories (4, 23). In this report, we have analyzed the intracellular maturation of ASFV in these replication sites and the structural contribution of mature products derived from polyprotein pp220. Fine immunocytochemical and morphological evidences indicate that ASFV polyprotein products are localized in an intermediate domain, referred to here as the core shell, between the nucleoid and the inner viral envelope. Quantitative analyses showed that structural proteins p150, p37, p34, and p14 are present in equimolar moieties in the virus particle, accounting for about one-fourth of its protein content. Our results indicate that ASFV polyprotein plays an important role in the viral morphogenesis which might be similar to that of the matrix proteins of other viruses.

MATERIALS AND METHODS

Cells and viruses. Vero cells (ATCC CCL81) were cultured in Dulbecco's modified Eagle's medium supplemented with 10% newborn calf serum, which was reduced to 2% during viral infection. Swine alveolar macrophages, obtained by bronchoalveolar lavage, were maintained and infected in Dulbecco's modified Eagle's medium with 10% newborn calf serum. ASFV strain BA71V, adapted to grow in Vero cells, has been previously described (14). Highly purified ASFV was obtained by Percoll equilibrium centrifugation (7).

Antibodies. Monoclonal antibody 18H.H7, against proteins pp220 and p150, as well as rabbit polyclonal anti-p150, anti-p37/p14, and anti-p34 sera, which also recognize the precursor form pp220, have been characterized previously (28, 33). Monoclonal antibody 19B.A2, against protein p72, has been described before (28). The anti-DNA immunoglobulin M (Ac 30-10) was obtained from Boehr-

* Corresponding author. Phone: 34 1 397 84 36. Fax: 34 1 397 84 90. E-mail: Evinuela@mvax.cbm.uam.es.

† Present address: Laboratory of Genetics, University of Gent, 9000 Gent, Belgium.

inger Mannheim. The rabbit antiserum against protein p63 (31) was kindly provided by S. Kornfeld.

Metabolic labeling, immunoprecipitation, and electrophoretic analysis. [^{35}S]methionine-labeled extracellular virus was purified as previously described (7). High-resolution two-dimensional (2-D) gel electrophoresis was performed essentially as described by Bravo (3), with slight modifications (1). Sodium dodecyl sulfate (SDS)-polyacrylamide gradient slab gels (7 to 20%) were used for both second-dimensional gels and conventional SDS-polyacrylamide gel electrophoresis. Isoelectric points (pI) were estimated with a set of pI markers of Bio-Rad.

For immunoprecipitation experiments, radiolabeled virus was dissociated in radioimmunoprecipitation assay buffer (0.01 M Tris-HCl [pH 7.5], 0.15 M NaCl, 1% sodium deoxycholate, 1% Nonidet P-40, 0.1% SDS) and incubated with the different anti-pp220 sera for 2 h at 4°C, followed by protein A-Sepharose for 30 min. After extensive washing with radioimmunoprecipitation assay buffer, immune complexes were solubilized by heating for 1 h at 37°C in lysis buffer (9.8 M urea, 2% Nonidet P-40, 2% ampholytes [pH 7 to 9; Pharmacia LKB] 0.1 M dithiothreitol) for 2-D gel electrophoresis.

For quantification of radiolabeled proteins, relevant bands and spots were identified by examining the exposed X-ray film. Then proteins were excised from dried gels, immersed in scintillation liquid, and counted for 5 min in an LKB 1209 Rackbeta counter. Measurements were normalized by taking into account the number of methionine residues of the corresponding proteins. Quantitation of Coomassie blue-stained proteins was carried out with a computing densitometer (model 300A; Molecular Dynamics). The relative amounts of the selected proteins were normalized with respect to their theoretical molecular weights.

Subcellular fractionation and Western blotting. Subcellular fractionation was performed as described previously (26), with slight modifications. All steps were performed at 4°C. ASFV-infected Vero cells were resuspended at 18 h postinfection (hpi) in a homogenization buffer containing 20 mM HEPES (pH 7.4), 0.28 M sucrose, 2 mM EDTA, and 1 mM phenylmethanesulfonyl fluoride and then disrupted by N_2 cavitation for 10 min at 250 lb/in^2. Cell breakage was monitored by phase-contrast microscopy. Extracts were centrifugated at 1,000 × *g* for 5 min to sediment nuclei and large particulate material. The 1,000 × *g* supernatant fraction was further fractionated into membrane/particulate and soluble fractions by centrifugation at 150,000 × *g* for 30 min.

Analysis of subcellular fractions was performed by Western immunoblotting. Equivalent amounts of nuclear, cytosolic, and membrane/particulate fractions were electrophoresed and subsequently transferred onto nitrocellulose (0.2-μm pore size; Renner) with a Mini Protean II apparatus (Bio-Rad) according to the manufacturer's instructions. Membranes were blocked in phosphate-buffered saline (PBS) with 0.1% Tween 20 and 3% dry milk powder for 30 min and then incubated with the indicated antibodies for 1 h. Protein detection was carried out with peroxidase-conjugated secondary antibodies and an electrochemoluminescence system (ECL system; Amersham Life Science) according to the manufacturer's recommendations.

Light microscopy. Vero cells were grown to ca. 70% confluency in chamber slides (Lab-Tek; Nunc) and then infected with the ASFV strain BA71V at 1 PFU per cell. The cells were fixed after the indicated times with methanol at −20°C for 5 min. All incubations for immunofluorescence labeling were carried out in PBS. Cells were labeled with the primary antibody (monoclonal antibody 18HH7; 1:10 dilution in PBS) in 0.1% bovine serum albumin at 37°C for 1 h, rinsed three times for 5 min, and incubated with fluoresceinated goat anti-mouse immunoglobulin G (Tago, Inc., Burlingame, Calif.) with 0.1% bovine serum albumin at 37°C for 1 h. Nuclear and viral DNA were visualized by staining with 5 μg of bisbenzimide (Hoeschst 33258; Sigma) per ml of PBS for 5 min. The coverslips were mounted on glass slides by using Moviol and examined with an Axiovert fluorescence microscope (Carl Zeiss, Inc., Oberkochen, Germany) and photographed with Kodak film TMAX (ASA 400).

Electron microscopy. In general, Vero cells or swine macrophages were infected with more than 25 PFU per cell. Vero cells were detached from the tissue culture dish with proteinase K (50 μg/ml; Merck) on ice for 2 to 3 min. Swine macrophages were removed with 0.01% EDTA for 15 min. For conventional Epon embedding, samples were first fixed for 60 min in 2% glutaraldehyde and 2% tannic acid in cacodylate buffer (pH 7.4) and then postfixed with 1% aqueous osmium tetroxide for 30 min. All incubations were performed at room temperature. For immunoelectron microscopy, infected cells were usually processed by freeze substitution. Samples were fixed for 60 min with 4% paraformaldehyde in 0.1 M phosphate buffer (pH 7.2) on ice and cryoprotected with 30% glycerol for 30 min. Specimens were rapidly frozen in liquid propane (−180°C) and stored in liquid nitrogen before use. Freeze substitution was carried out at −90°C in methanol supplemented with 0.5% tannic acid for 40 h. Dehydration continued with pure methanol by raising the temperature to −35°C at a rate of 3°C/h. Finally, the samples were embedded in K4M at −35°C and polymerized by irradiation with UV light. In some cases, we used a conventional procedure for Lowicryl embedding, which was carried out as described by Carlemalm et al. (6). For postembedding labeling, ultrathin sections (50 to 90 nm, depending on the experiment) were floated for 5 min on drops of PBS with 1% egg albumin. Then the grids were incubated for 1 h with the first antibodies (anti-p150, anti-p37/p14, and anti-p34 at 1:10 to 1:20 dilutions in PBS with 1% egg albumin), rinsed with PBS, and incubated for 45 min with protein A-gold complexes (5, 10, or 15 nm; BioCell Research Laboratories, Cardiff, United Kingdom) diluted 1:20 in PBS with 1% egg albumin. In the case of the anti-DNA monoclonal antibody (1:2 dilution), the grids were incubated with goat anti-mouse antibodies conjugated to colloidal gold (10 or 15 nm) diluted 1:20 in the same buffer.

For quantification, electron micrographs of virus sections showing a hexagonal outline were analyzed at a magnification of ×100,000. Radial distribution of gold particles was calculated by determining, for each virus section, the distance of each gold granule to the center of the virus. Specimens were examined at 80 kV in a Jeol 1010 or Jeol 1200X electron microscope.

RESULTS

Assembly of ASFV. To study the assembly pathway of ASFV, we carried out an electron microscopic (EM) analysis of infected Vero cells during the late phase of infection (8 to 24 hpi). ASFV assembly occurs in discrete cytoplasmic areas usually close to the nucleus called viral factories (4) (Fig. 1A). These replication sites contain abundant electron-dense membranous structures as well as assembling virions in all different stages of virus formation (4, 23). The disposition of the viral membranes is highly variable: irregular and parallel arrangements without apparent continuities with cellular organelles could be detected in the same viral factory (23) (Fig. 1B). However, viral membranes were often found in direct continuity with assembling virions (Fig. 1B). This observation became even more evident when serial sections of the membranous structures were analyzed. As shown in Fig. 1C, viral membranes appeared as laminar structures that eventually folded to form polyhedral immature virions. We conclude that these membranous structures represent the precursor forms of ASFV particles.

We next analyzed the fine structure of the different intermediate stages of the maturation of ASFV. Figure 2 summarizes the likely sequence of the assembly process. As shown in Fig. 2A, viral membranes became polyhedral structures by the progressive formation of the capsid on their convex surface. The capsid, a layer of regularly arranged subunits displaying an hexagonal pattern (8), therefore represents the outermost layer of the intracellular virus. Underneath the concave surface of the envelope, two distinct domains appeared to form consecutively. First formed was a thick layer of about 30 nm which seemed subdivided in an apparently symmetrical fashion by a thin and electron-dense layer (Fig. 2B and C). Many images of this intermediate domain showed also a regular array of globular subunits of an average length of 10 nm to both sides of the thin layer (Fig. 2B). However, this particular organization was less evident in images of extracellular mature virions (Fig. 2G), which suggests a further maturation process within this domain. We will refer to this structure as the core shell to distinguish it from the electron-dense central component of about 80 nm (Fig. 2E), which we consider the nucleoid proper (see below). Differentiation of the viral nucleoid was detected only in virus particles whose outer layers were almost completed (Fig. 2D and E). Moreover, we did not detect isolated nucleoids in the replication areas. Taken together, these observations indicate that nucleoid formation is, as in the case of other DNA viruses, a late stage in the viral assembly. Finally, virus particles are released to the extracellular space by budding from the plasma membrane (Fig. 2F) as described previously by Breese and DeBoer (4). Identical results were obtained with infected swine macrophages, the natural target cells of ASFV (not shown).

In summary, ASFV morphogenesis is a multistep process which, according with our EM observations, leads to the consecutive assembly of at least five distinct structural domains: the core composed of a dense nucleoid surrounded by a thick layer (the core shell), the inner envelope, the capsid, and finally the external lipid envelope (Fig. 2G).

Relative abundance and stoichiometry of polyprotein pp220 products within the virus particle. The previous results pro-

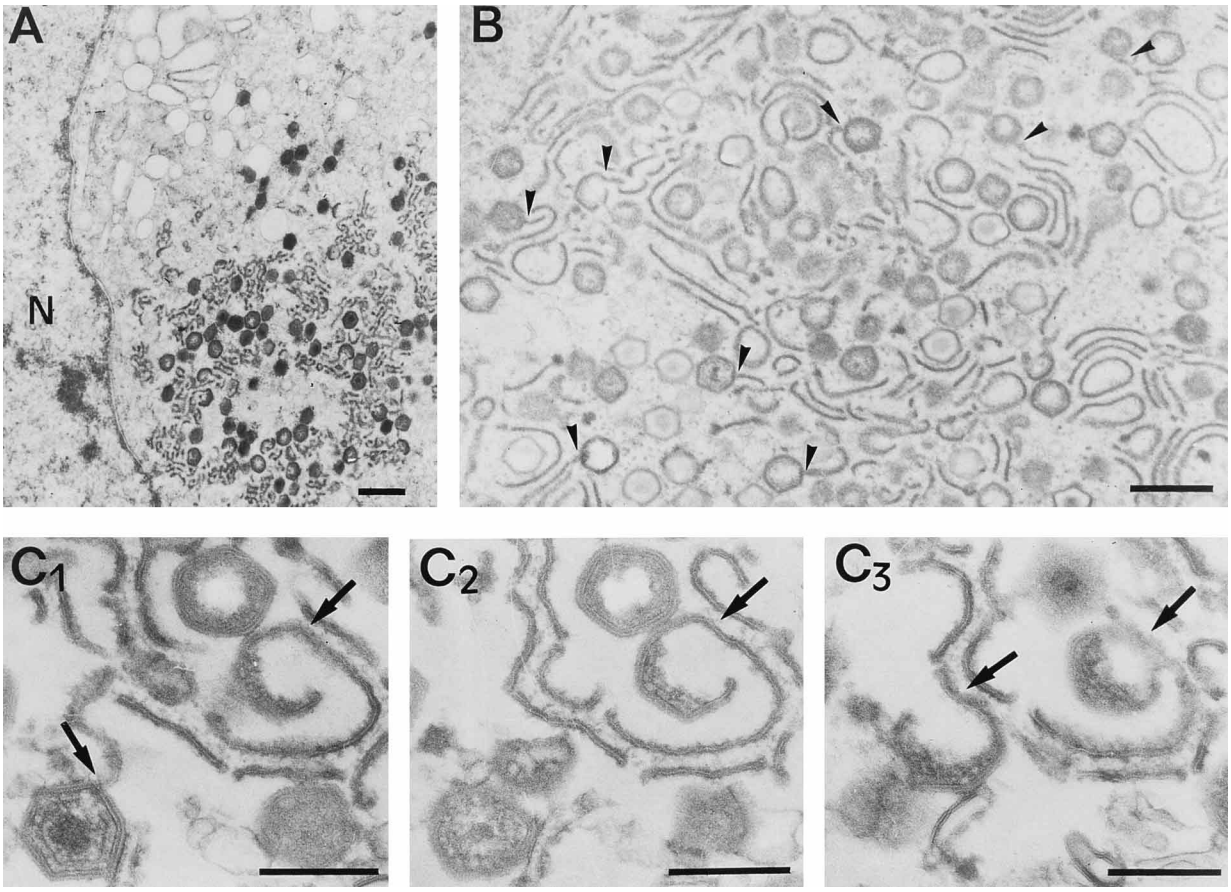

FIG. 1. Ultrathin Epon sections of viral factories in ASFV-infected Vero cells. (A) Virus assembly takes place in discrete cytoplasmic areas close to the nucleus (N), which contain abundant electron-dense membrane-like structures. (B) These structures are frequently found in direct continuity with assembling viruses (arrowheads). (C) Set of serial sections of a viral factory. Viral membranes appear like laminar curved structures which eventually fold in polyhedral assembling virions (arrows). Bars: (A and B) 500 nm; (C) 200 nm.

vided us with an appropriate framework to analyze the role of polyprotein pp220 in the virus assembly. The largest gene of the ASFV genome (CP2475L) encodes a polyprotein, named pp220, which is posttranslationally processed to give rise to four structural components of the virus particle, proteins p150, p37, p34, and p14 (33) (Fig. 3A). To determine their contribution to the structure and protein composition of the virus particle, we first analyzed their stoichiometry and relative abundances. For this purpose, highly purified ASFV particles labeled with [^{35}S]methionine were obtained by Percoll equilibrium centrifugation (7). Virus proteins were separated by 1-D and 2-D gel electrophoresis (Fig. 3B, panels 1 and 2), and polypeptides p150, p37, p34, and p14 were mapped in the gels after immunoprecipitation with monospecific antisera (Fig. 3B, panel 3). The radioactivity of each polypeptide was determined by isotopic counting of the corresponding excised pieces of 2-D gels, and the data were corrected by taking into account the number of methionine residues of each protein (33). Since protein p150 was usually poorly focused in the limit of the 2-D gels (1) (Fig. 3B, panels 2 and 3), its quantitation was carried out in 1-D gels and then compared to that of protein p37. The results, summarized in Fig. 3C (^{35}S-Met column), showed that the structural proteins derived from polyprotein pp220 are present in the virus particle in an essentially equimolecular stoichiometry. In other approach, we quantified the polyprotein products by densitometric analysis of 1-D and 2-D gels stained with Coomassie blue. The results, normalized in this case with respect to the theoretical molecular weight of each protein (33), showed again very similar molar proportions of the polyprotein products except for p150, the level of which was found to be about one-half of that of the other proteins (Fig. 3C, Coomassie column). Considering that radioactive quantitation is a more precise method than densitometry of stained proteins, we interpret this result to be a consequence of the anomalous staining of p150.

Densitometric analysis of 1-D gels also provided a way to estimate the relative abundances of the polyprotein products. Polyprotein products p150 and p37 and, as a reference, the major structural protein p72 were measured (Fig. 3C, % column). Proteins p34 and p14 were not quantified due to the heterogeneity of the bands corresponding to both proteins (compare 1-D with 2-D gels in Fig. 3B, panels 1 and 2). Assuming an equimolar stoichiometry for all polyprotein products (see the legend to Fig. 3C), densitometric analysis of Coomassie blue-stained 1-D gels revealed that they collectively represent about 25% of the protein mass of the virus particle (% corr. column). As a reference, the major capsid protein p72 (22) was found to constitute ca. 32% of the total protein content.

Although the protein mass of ASFV has not been reported, it can be estimated by using the published values for the DNA/protein ratio, 0.18 (7), and the molecular mass of the virus DNA, about 100×10^6 Da (39). With this approach, the

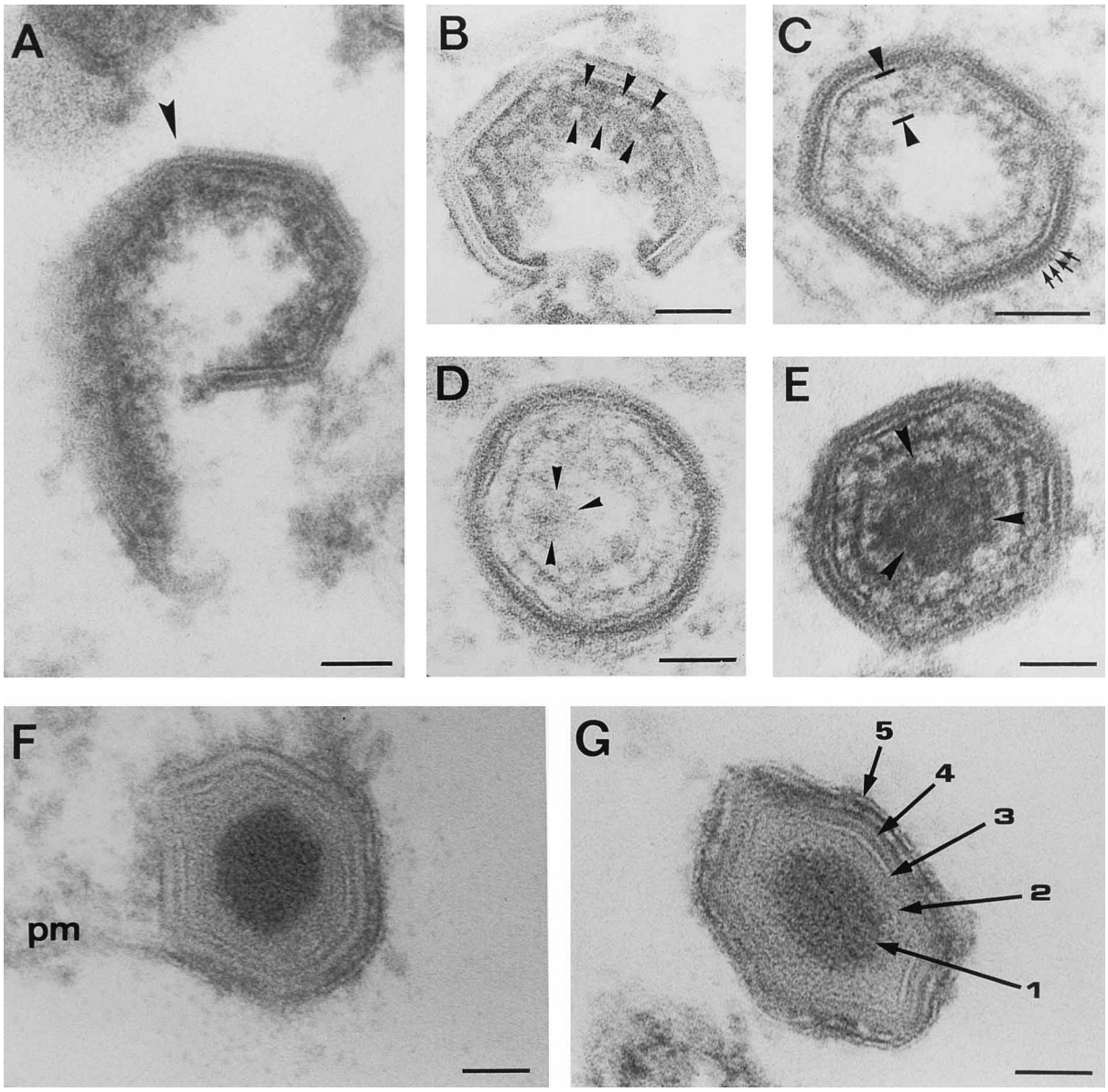

FIG. 2. Ultrathin Epon sections of selected intermediate and mature viral forms illustrating the possible assembly process. The membrane-like structures become polyhedral forms after progressive formation of the capsid on their convex surface (A to C). The arrowhead in panel A and the small arrows in panel C point to the capsomers on the surface of the intracellular virus particles. Beneath the envelope, a thick layer of about 30 nm, referred to as the core shell, is built prior to nucleoid formation (B and C). The core shell (arrowheads in panel C) is apparently formed by two regular arrays of globular subunits (arrowheads in panel B) separated by a thin and electron-dense layer. The intracellular virions are completed in the viral factories after nucleoid formation (D and E, arrowheads). Finally, the viral particles are released to the extracellular space, acquiring an additional envelope (F) by budding at the plasma membrane (pm). Panel G shows an extracellular mature virion. Arrow numbers indicate the following domains: 1, nucleoid; 2, core shell; 3, inner envelope; 4, capsid; 5, outer envelope. Note that the external envelope surrounds loosely the capsid. Bars, 50 nm.

protein content of ASFV was found to be about 555×10^6 Da, which tentatively suggest a copy number for each polyprotein product of about 500 molecules per virion. In summary, these results show a very significant contribution of polyprotein pp220 to the ASFV structure.

Intracellular distribution of polyprotein pp220. The ASFV gene CP2475L is regulated by a late viral promoter since polyprotein expression occurs at late times after infection, from 8 to 10 hpi onward, and is inhibited by cytosine arabinoside, an inhibitor of ASFV DNA replication (1). To analyze the intracellular localization of polyprotein pp220 during the late phase of infection, we carried out immunofluorescence experiments with a monoclonal antibody, 18H.H7, which recognizes both pp220 and the mature product p150 (28). The first detectable signal, at about 8 hpi, was located in discrete cytoplasmic areas close to the nucleus, which were identified as viral factories by DNA staining with bisbenzimide (Fig. 4). At later times of infection, labeling of the replication sites became more prominent and occupied larger areas of the cytoplasm. Finally, from about 16 hpi, anti-pp220 antibodies additionally labeled punctate structures scattered throughout the cytoplasm, most probably representing single virus particles migrating toward the cell surface.

In another approach, we analyzed the subcellular distribu-

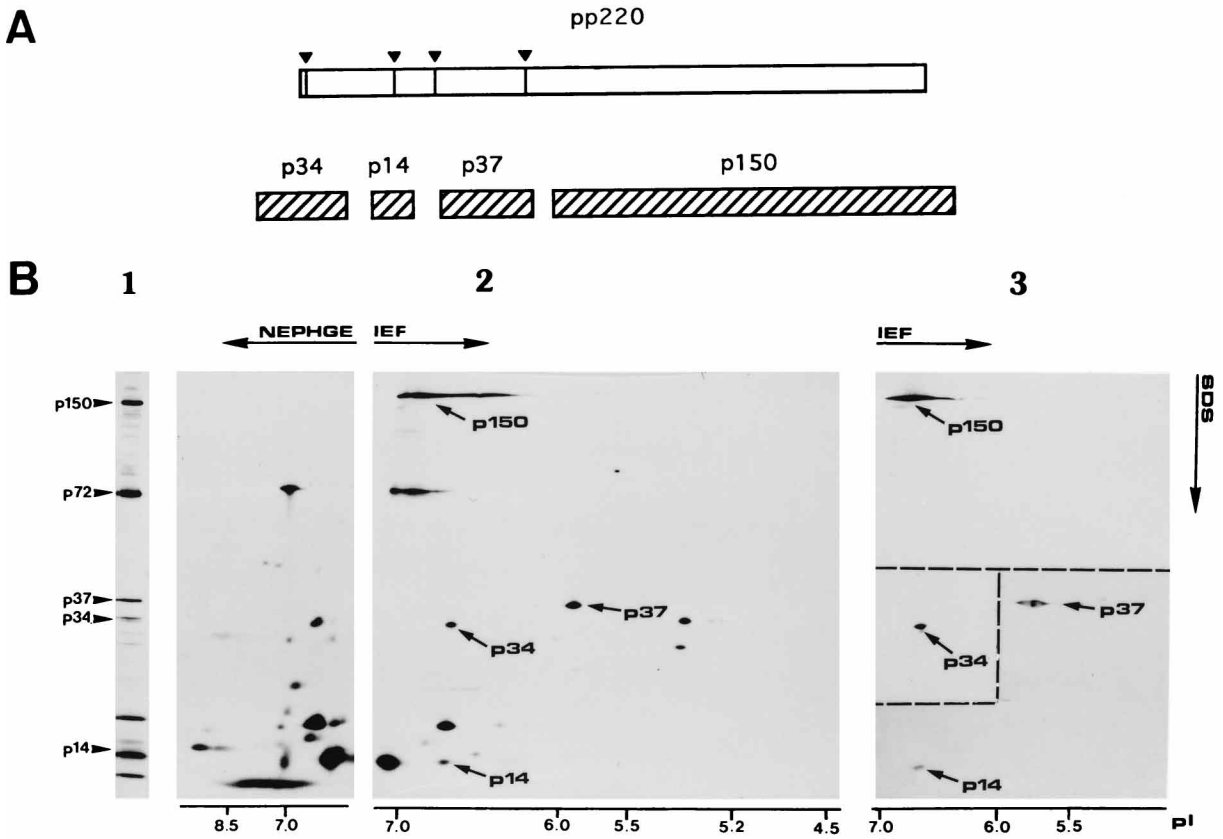

C

Protein	M	Met	Stoichiometry		Relative abundance	
			^{35}S-Met	Coomassie	%	% corr.
p150	181,133	43	1.0 ± 0.1	0.5 ± 0.2	8.8 ± 1.6	16.4 ± 3.0
p37	41,488	10	1	1	4.1 ± 0.9	3.8 ± 0.8
p34	36,349	3	1.1 ± 0.1	0.9 ± 0.2	—	3.3 ± 0.7
p14	17,768	3	1.2 ± 0.1	1.0 ± 0.2	—	1.6 ± 0.3
p72	73,096	8	5.4 ± 0.8	5.1 ± 1.7	34.4 ± 6.2	31.6 ± 5.7

FIG. 3. Stoichiometry and relative abundance of proteins p150, p37, p34, and p14 in the virus particle. (A) Processing map of polyprotein pp220. Triangles indicate the cleavage sites (Gly-Gly-X) in the ASFV polyprotein. The structural proteins generated after proteolytic processing are represented by hatched boxes. (B) Gel mapping of the polyprotein products. Highly purified ASFV particles labeled with [^{35}S]methionine were analyzed by both conventional SDS-polyacrylamide gel electrophoresis (panel 1) and 2-D gel electrophoresis (panel 2; nonequilibrium pH gradient electrophoresis [NEPHGE] and isoelectric focusing [IEF]). Localization of polyprotein products was carried out by immunoprecipitation of labeled virus extracellular particles with antisera against proteins p150, p37/p14, and p34 (panel 3). pI values are indicated as a reference below the 2-D gels. (C) Quantitative analysis of the polyprotein products. The stoichiometry of the polyprotein products in the virus particle was determined by isotopic counting of ^{35}S-labeled proteins (three determinations) as well as gel densitometry of Coomassie blue-stained proteins (four determinations). Proteins p37, p34, and p14 were analyzed directly from 2-D gels. Quantitation of protein p150 was made on 1-D gels due to its deficient focusing in 2-D gels. Stoichiometry data are normalized to those for protein p37, which was well resolved in both 1- and 2-D gels. Estimation of relative abundances (% column) was performed by densitometric scanning of Coomassie blue-stained 1-D gels (six determinations). As proteins p34 and p14 cannot be estimated in these gels because of heterogeneity of the bands, their relative abundances were calculated assuming an equimolar stoichiometry for all the polyprotein products (% corr. column). As a reference, quantitation of the major capsid protein p72 is also shown. M, molecular weight.

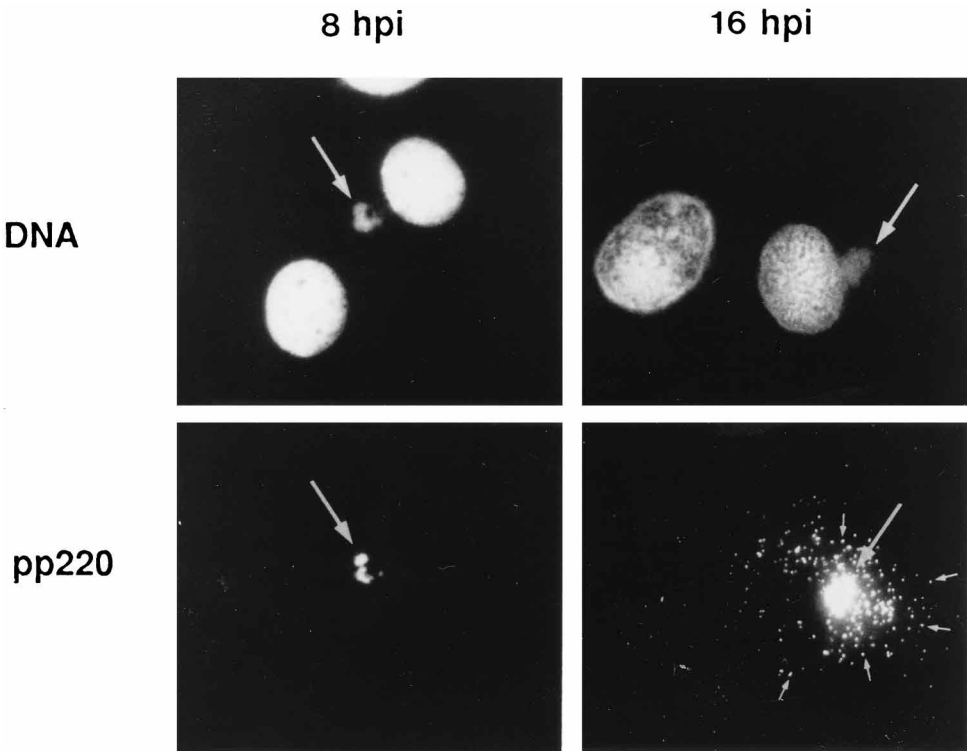

FIG. 4. Immunofluorescence microscopy of polyprotein pp220 in ASFV-infected cells. ASFV-infected Vero cells were fixed at the indicated times of infection and labeled with a fluorescent DNA dye (Hoeschst 33258; upper panels) and with a monoclonal antibody against pp220/p150 (18H.H7) followed by a fluorescein-conjugated goat anti-mouse antibody (lower panels). Anti-pp220 labeling colocalizes with the area of the viral factories as defined by DNA staining (large arrows point to equivalent positions). Additionally, strong labeling was detected at later times (16 hpi) on punctate structures scattered throughout the cytoplasm (small arrows), most probably corresponding to single virus particles.

tion of polyprotein pp220 by fractionation experiments. ASFV-infected Vero cells were disrupted at 18 hpi by nitrogen cavitation and fractionated as described in Materials and Methods. The distribution of pp220 was analyzed by Western blotting with an anti-pp220/p150 serum. As shown in Fig. 5, most of the polyprotein and of the mature product p150 was detected in the membrane/particulate fraction, although a minor proportion was also present in the nuclear fraction. In contrast, the analysis of the major capsid component p72 revealed a significant presence in the cytosolic fraction as well as in the membrane/particulate fraction. As a control, the subcellular distribution of protein p63, a membrane marker of the endoplasmic reticulum (ER) (31), showed a pattern very similar to that of proteins pp220 and p150. These results suggest that polyprotein pp220 is associated with membranes. However, as virus particles cosediment with the membrane components under the conditions used, it cannot be excluded that the presence of the polyprotein in the membrane fraction is due to its association with immature virions.

To examine in more detail the structural contribution of polyprotein pp220 to ASFV assembly, we carried out immunolocalization experiments at the EM level. Ultrathin Lowicryl sections of infected cells processed at late times postinfection were incubated with antibodies against different regions of the polyprotein and subsequently with protein A-gold. No qualitative difference was detected between the different sera (see below). Postembedding labeling was essentially located on the replication areas (Fig. 6) as well as on virus particles spreading throughout the cytoplasm (not shown), which is consistent with the labeling pattern seen by immunofluorescence microscopy. Gold particles were found associated with all morphologically detectable forms of ASFV from the precursor viral membranes onward (Fig. 6A), thus indicating an early role for polyprotein pp220 in viral assembly. Antibodies to pp220 significantly labeled mature virions as well as assembling particles without nucleoid (Fig. 6), preferentially on their concave surface. Additionally, significant labeling was detected in close proximity to precursor viral membranes (Fig. 6A and C), an observation supported by preembedding labeling of infected cells (not shown). Taken together, subcellular fractionation and EM experiments suggest that pp220 is a membrane-associated protein.

Subviral localization of the polyprotein products. Figure 7A shows the labeling pattern obtained with the different antibodies to pp220 on selected sections of intracellular full virions present in the assembly sites. For all of the sera, a radial

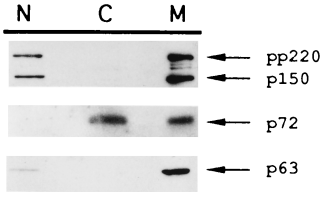

FIG. 5. Subcellular distribution of polyprotein pp220 in ASFV-infected cells. Infected cells were disrupted at 18 hpi by N_2 cavitation and fractioned as described in Materials and Methods. Equivalent amounts of nuclear (N), cytosolic (C), and membrane/particulate (M) fractions were analyzed by Western blotting with a monospecific antiserum to pp220/p150, a monoclonal antibody (19B.A2) to the major capsid protein p72, and a polyclonal serum against p63, a membrane ER protein.

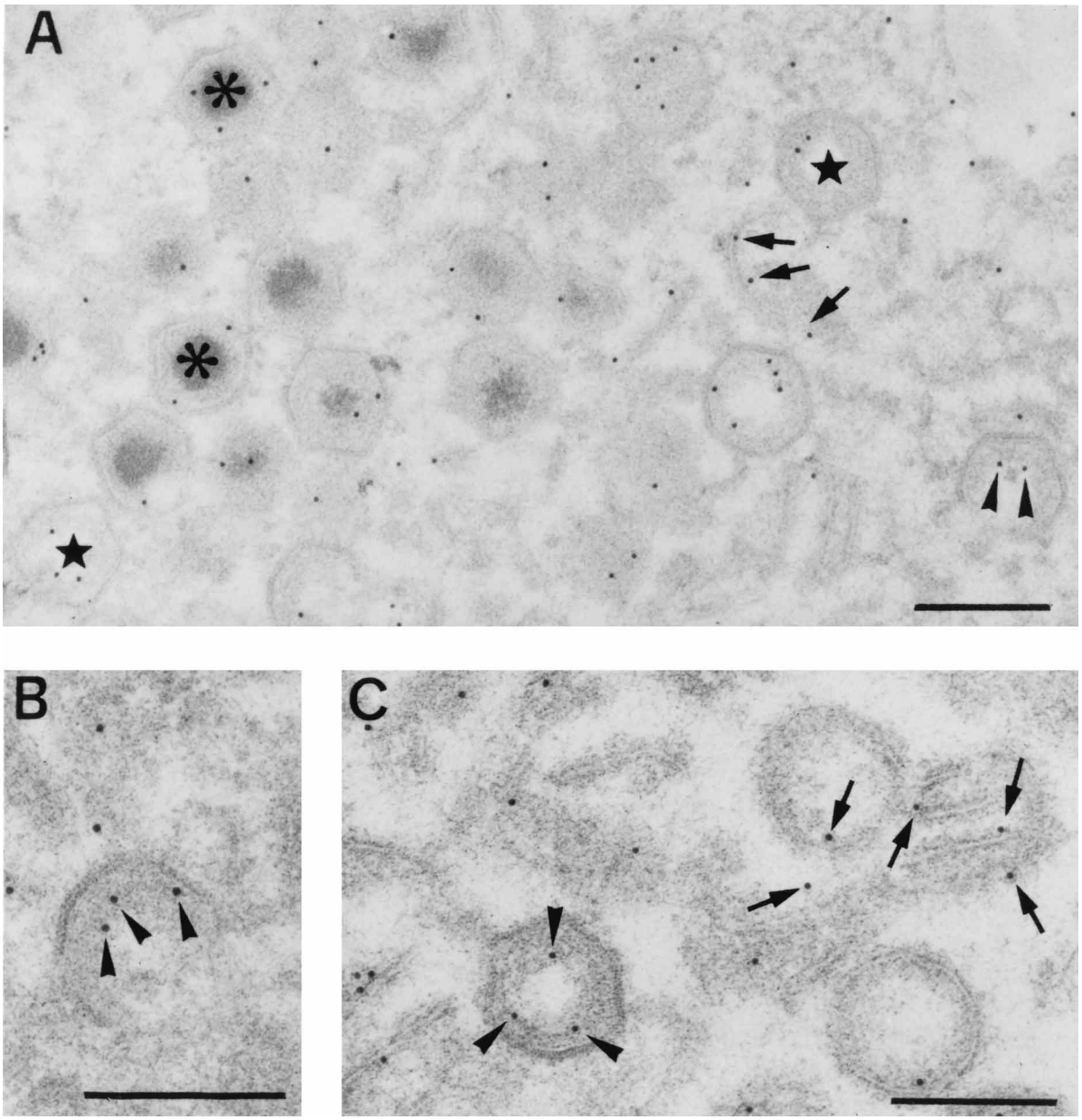

FIG. 6. Immunoelectron microscopy with anti-pp220 antibodies in ASFV-infected cells. Infected Vero cells were fixed at 18 hpi and processed by freeze substitution. Ultrathin Lowicryl sections were incubated with anti-p150 (A), anti-p34 (B), or anti-p37/p14 (C) antibodies followed by protein A-gold (10 nm). All antibodies strongly labeled the region of the viral factories, and no major qualitative differences were found between them. Gold particles decorated both mature (asterisks) and immature (stars) virions (A). Note the labeling associated with the concave surface of assembling virions (arrowheads in panels A to C) and in close proximity to viral membrane-like structures (arrows in panels A and C). Bars, 200 nm.

distribution of gold particles (10 nm) was evident on the core shell encompassing the electron-dense nucleoid. Such distribution strongly suggests an intermediate localization of the polyprotein products in the virus particle. However, as the anti-pp220 sera recognize both the precursor form and the mature products (33), we cannot exclude an incomplete processing in a certain proportion of the intracellular virions. Therefore, we performed immunogold labeling on sections of highly purified extracellular ASFV particles, which lack precursor pp220 (7, 33). To finely determine the distribution of gold particles, we used in this approach very thin sections (around 50 to 60 nm, compared with 70 to 90 nm for normal sections) and gold particles of around 5 nm and omitted the tannic acid treatment to evidence more clearly the immunogold complexes over the virions. As shown in Fig. 7B, the results were similar to those of the previous experiment. Furthermore, a higher labeling efficiency was obtained, probably related to the use of a smaller gold probe and the subsequent reduction of steric impediments to the antigen-antibody interactions. The radial distributions of the different polyprotein products, expressed in nanometers, were 60 ± 10 (anti-p150, n = 107 gold granules counted), 52 ± 14 (anti-p37/p14, n = 123), and 55 ± 9 (anti-p34, n = 100). Such results are in good accordance with their localization in the core shell, radial dimensions of which are around 40 nm (inner) and 70 nm (outer).

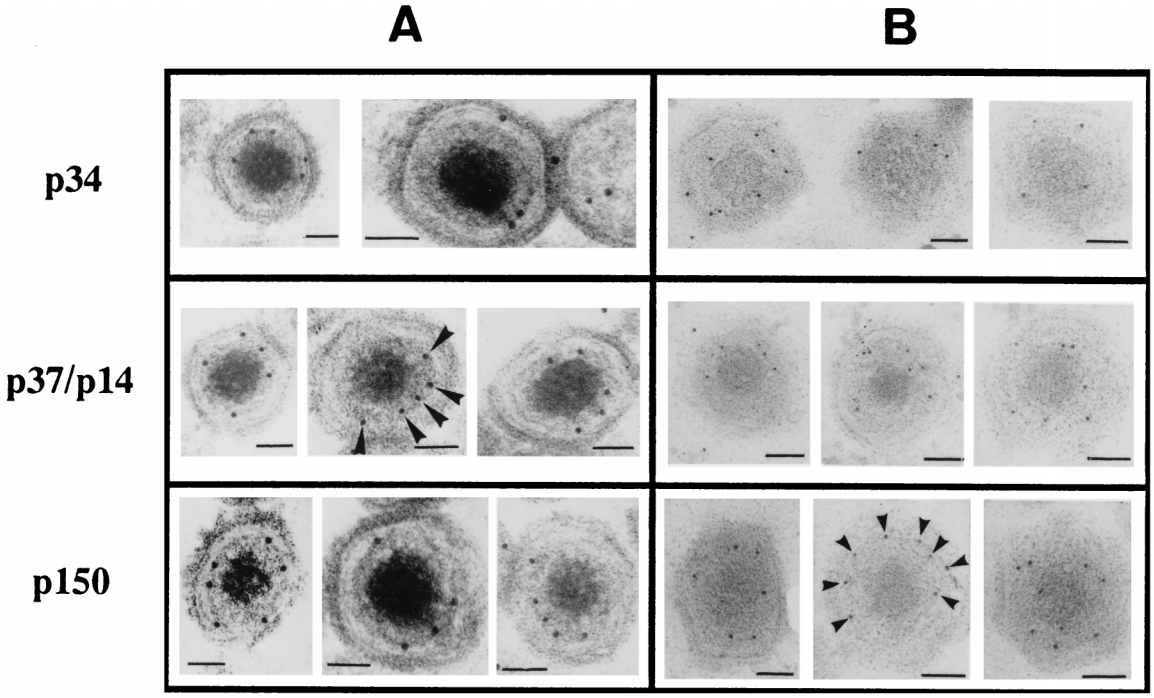

FIG. 7. Subviral localization of structural proteins derived from polyprotein pp220. Lowicryl sections of intracellular full virions within viral factories (A) or purified extracellular virus particles (B) were incubated with anti-p34, anti-p37/p14, and anti-p150 sera followed by protein A-gold (10 nm [A] and 5 nm [B]). Arrowheads point to the radial distribution of gold granules within the core shell, the intermediate domain between the viral nucleoid and the external layers. Bars, 50 nm.

Immunocytochemical identification of the viral nucleoid. Morphological and immunological evidences indicate that the core shell is a domain structural and biochemically distinct from the electron-dense nucleoid, which is presumably the DNA-containing domain. To demonstrate that the viral genome is confined into this central structure, we labeled sections of infected cells and purified virions with a monoclonal anti-DNA antibody (29). As shown in Fig. 8A, specific labeling was detected in the cellular nucleus, especially on the peripheral areas of condensed chromatin, and in the viral factories. Gold particles in the replication areas were mainly associated with full virions, although labeling efficiency was usually low. A similar result has been obtained with other viruses, and it is likely due to the strong association of core proteins with the viral genome (25, 34). Despite this, labeling of purified virions clearly showed that most of the gold particles (78%, $n = 150$) decorated the electron-dense nucleoid (Fig. 8B and C), thus confirming the architecture proposed for the internal structure of ASFV.

DISCUSSION

ASFV assembly. Very little is known about the assembly pathway of ASFV, which probably has hampered efforts to determine the structural functions of most of the virus components. In this study, we used EM techniques to understand the intracellular maturation of ASFV and the role of the structural polypeptides derived from polyprotein pp220. Viral assembly takes place in discrete cytoplasmic regions close to the nucleus called viral factories (4, 23). These replication areas contain abundant membranous structures whose origin has not been established (23). We considered the appearance of these viral membranes as the first indication of viral assembly, as judged by the continuities detected between these structures and assembling virions. Viral membranes seem to become polyhedral immature particles by the progressive formation of the capsid on its convex surface. This process might be analogous to the formation of the crescent-shaped membranes of the poxviruses, which are also covered by a brush-like array of electron-dense spicules on their convex surface (11). Our EM observations also indicated that ASFV, like poxviruses, does not acquire its first envelope by a budding process at a cellular organelle. This mechanism implies the acquisition of a single membrane and, concomitantly, a change of compartment of the virus particle. ASFV assembly takes place in the viroplasm, a cytosolic environment, and we rarely found virus particles in the lumen of cytoplasmic compartments (see below). In this context, it has been recently proposed that the intracellular mature vaccinia virus (IMV) becomes enwrapped by a membrane cisterna derived from the intermediate compartment, a specialized region of the ER (34). According to this model, the lipid envelope of IMV consists of two unit membranes so tightly juxtaposed that they appear usually as a single membrane (27, 34). A similar model could explain the topology of ASFV assembly and the apparent existence of a single membrane below the capsid of the virus particles.

Underneath the lipid envelope, two different domains appear to be consecutively formed: first the core shell, a thick protein layer of about 30 nm which apparently consists of two sets of regularly arranged globular subunits separated by a thin and electron-dense layer; and then the viral nucleoid, an electron-dense structure of about 80 nm. According to our EM studies, the encapsidation of the viral genome could represent a late event in the ASFV assembly. A similar proposal has been recently reported by Brookes et al. (5). However, these authors suggest that the viral nucleoid might be formed prior to its insertion into a partly formed empty capsid. We have not detected proper isolated nucleoids in the assembly sites, which

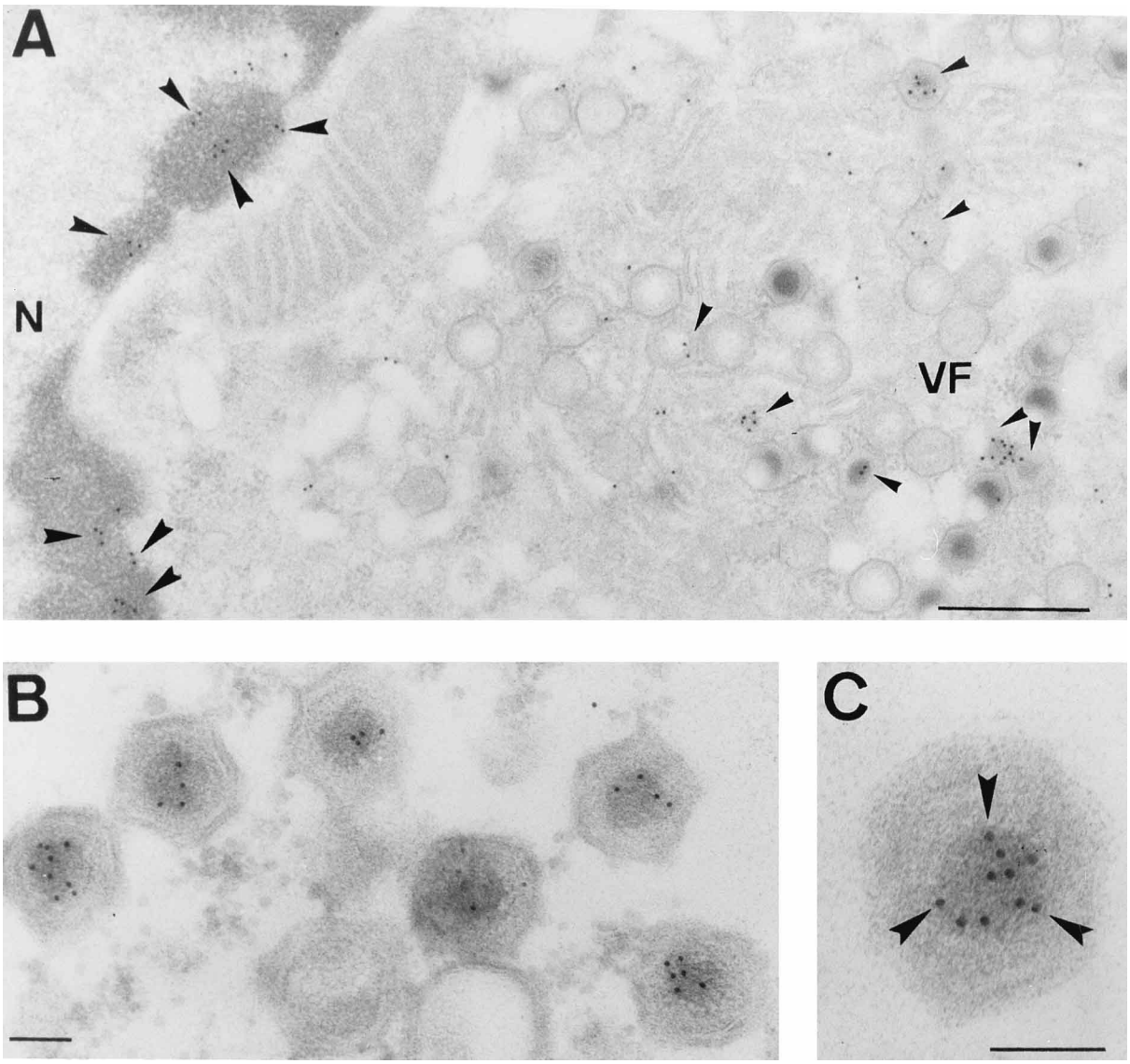

FIG. 8. Immunolocalization of the viral nucleoid with monoclonal anti-DNA antibodies. (A) Localization of both cellular and viral DNA in a Lowicryl section of an ASFV-infected cell (18 hpi) processed by freeze substitution. Labeling was performed with monoclonal antibody Ac 30-10 to DNA followed by secondary antibodies coupled to 15-nm gold particles. Note the labeling of the condensed chromatin regions (large arrowheads) in the periphery of the nucleus (N) as well as on the area of a viral factory (VF), mainly within the virions (small arrowheads). (B and C) Labeling of viral DNA within purified virions obtained by Percoll centrifugation. Most of the gold particles (10 nm) are present in the central and electron-dense nucleoid (arrowheads). Bars: (A) 500 nm; (B and C) 100 nm.

suggests that the nucleoprotein material is condensed after its insertion into the virus particle such as indicated in Fig. 2D. Nevertheless, further experiments are necessary to determine the precise mechanism of genome packaging.

Extracellular virions posses an additional lipid envelope acquired by budding from the plasma membrane, as previously reported by Breese and DeBoer (4). The multistep assembly process described in the present study leads therefore to a structural model for ASFV consisting of at least five concentric domains (Fig. 2F). Such a model is divergent in some aspects from others previously reported. For example, Schloer (30) and Arzuza et al. (2) include an additional membrane between the capsid and the external envelope. Such a membrane would be the outermost layer of the intracellular particles. With one exception, we have no evidence for such a membrane. Occasionally, we have seen cytoplasmic virus particles in the lumen of cellular membrane vesicles. These intracellular virions possess an additional membrane surrounding the capsid and thus are indistinguishable from the extracellular particles. Our interpretation is that they are endocytosed extracellular virions or intracellular virions which have budded into some cellular compartment. In this respect, a close inspection of micrographs of intracellular ASFV particles reported by Arzuza et al. (2) reveals that they are clearly in the luminal space of cytoplasmic vesicles, an infrequent circumstance according to our study and previous work (4, 5, 23).

Our model also establishes two functionally distinct domains in the core structure of ASFV. Differentiation between the core shell and the nucleoid is supported not only by ultrastructural analysis of assembling and mature virions but also by immunocytochemical data. Thus, while the central structure was specifically labeled with anti-DNA antibodies, the outer

shell was found to be constituted by the structural proteins derived from polyprotein pp220 processing. These results clarify the somewhat ambiguous definition of the core of previous models, based exclusively on morphological data (2, 8, 23, 30). Several functions can be attributed to the core shell. On the basis of its intermediate localization and its assembly way, the core shell may play a key role by its interaction with the nucleoprotein material as well as in membrane targeting. Besides its contribution to the structural integrity of the virions, the core shell might protect the viral genome from potentially destructive agents, such as nucleases, present in the extracellular environment or in the endosomes during the virus entry.

Role of polyprotein pp220. ASFV is an atypical DNA virus in that it uses polyprotein processing as a strategy to produce some of the major components of the virus particle, proteins p150, p37, p34, and p14 (33). In general, this mechanism of gene expression, usual in many positive-strand RNA viruses and retroviruses, appears to fulfill two functions during viral replication (13, 19). First, it serves as a mechanism to synthesize multiple functional gene products from genomic RNAs in a single transcription-translation event. The second role involves the maturation of structural proteins during the virus assembly process. In this report, we provide evidence that polyprotein pp220 plays an important structural role in ASFV morphogenesis. The expression of precursor pp220 takes place at late times after infection, from 8 to 10 hpi (1), in discrete cytoplasmic areas which were identified as viral factories by fluorescent DNA staining. At the EM level, antibodies to pp220 labeled all morphologically detectable forms of ASFV from the precursor viral membranes onward, thus indicating an early role of ASFV polyprotein in the virus assembly. However, since the antibodies to pp220 used in this work recognize both precursor and mature products, we could not correlate specific proteolytic events to identifiable stages of the ASFV assembly. Association of pp220 to membrane structures was additionally supported by subcellular fractionation experiments. Interestingly, polyprotein pp220 lacks obvious transmembrane domains and is not glycosylated despite the presence of several putative N-glycosylation sites in its amino acid sequence (33). Collectively, these results support the idea that pp220 is a cytosolic membrane-associated protein. In this context, it is noteworthy that polyprotein pp220 is cotranslationally myristoylated at the N-terminal glycine (33). Myristoylation functions as a membrane association signal for some cellular and viral proteins (17, 37). Thus, it is tempting to speculate that this covalent modification could play a similar role in the membrane targeting of polyprotein pp220.

Immunogold labeling with the different anti-pp220 sera was mainly associated with the concave surface of assembling virions, thus indicating that polyprotein products are integral components of the virus particle. Moreover, a fine determination of the radial distributions obtained in purified extracellular virions showed that the structural products derived from pp220 compose the core shell. In this regard, it should be mentioned that previous work from our laboratory localized protein p150 in the nucleoid and one vertex of the virus particle (9). This subviral localization was determined in predominantly immature cytoplasmic virions by using a monoclonal antibody which also recognized the nuclei from uninfected and infected cells. We have not observed such localization of p150 in the present study, performed with polyclonal antibodies in both immature and mature particles.

The structural contribution of proteins p150, p37, p34, and p14 is highly significant because together they account for about 25% of the total protein content of the virion. In this regard, it should be mentioned that capsid protein p72 (7, 22), the major component of the virus particle, constitutes about 32% of its protein mass. Interestingly, the polyprotein products were found in virtually equimolar amounts in the virus particles. This particular stoichiometry does not appear to be an obvious consequence of their initial expression as a precursor of higher molecular weight. The temporal regulation of ASFV polyprotein processing (33) and factors such as the efficiency at which products are cleaved or their different relative stabilities imply that certain proteins might accumulate faster and to a greater extent than others (13). Rather, our results suggest that the equimolar stoichiometry of ASFV polyprotein products is the result of a certain ordered structure in the virus particle. This is the case for picornaviruses such as poliovirus, whose capsid is composed of essentially identical amounts of four different polypeptides derived from the structural polyprotein P1 (21). Processing of P1 is concomitant with the viral assembly determining that mature proteins are coordinately assembled to build the morphological units of the capsid. Likewise, processing of pp220 could represent a maturation process associated with the formation of the core shell, triggering unidirectional changes which would allow new protein interactions, either within the domain or with the adjacent structures. In line with this idea, we suggest that polyprotein pp220 may function as an internal protein scaffold that mediates the interaction of the nucleoid with the outer layers, similarly to the matrix proteins of other enveloped viruses (18, 24, 36). Our next goal is to determine the precise role of proteolytic processing in the maturation of this complex DNA virus.

ACKNOWLEDGMENTS

We thank M. L. Salas and J. Salas for critical reading of the manuscript and I. Sandoval, R. Blasco, and R. García for helpful discussions. We are very grateful to S. Kornfeld for his generous gift of antibodies. We also thank C. San-Martin and M. Rejas for technical assistance and J. A. Pérez Gracia for skillful help with the photography work.

This study was supported by grants from the Dirección General de Investigación Científica y Técnica (PB93-0160-C02-01), the European Community (AIR-CT93-1332), and Fundación Ramón Areces.

REFERENCES

1. **Andrés, G., C. Simón-Mateo, and E. Viñuela.** 1993. Characterization of two African swine fever virus 220-kDa proteins: a precursor of the major structural protein p150 and an oligomer of phosphoprotein p32. Virology **194:** 284–293.
2. **Arzuza, O., A. Urzainqui, J. R. Díaz-Ruiz, and E. Tabarés.** 1992. Morphogenesis of African swine fever virus in monkey kidney cells after reversible inhibition of replication by cycloheximide. Arch. Virol. **124:**343–354.
3. **Bravo, R.** 1984. Two-dimensional gel electrophoresis: a guide for the beginner, p. 3–36. *In* J. E. Celis and R. Bravo (ed.), Two-dimensional gel electrophoresis of proteins: methods and applications. Academic Press, New York, N.Y.
4. **Breese, S. S., Jr., and C. J. DeBoer.** 1966. Electron microscope observation of African swine fever virus in tissue culture cells. Virology **28:**420–428.
5. **Brookes, S. M., L. K. Dixon, and R. M. E. Parkhouse.** 1996. Assembly of African swine fever virus: quantitative ultrastructural analysis *in vitro* and *in vivo*. Virology **224:**84–92.
6. **Carlemalm, E., R. M. Garavito, and W. Wiliger.** 1981. Resin development for electron microscopy and an analysis of embedding at low temperature. J. Microsc. **126:**123–143.
7. **Carrascosa, A. L., M. del Val, J. F. Santarén, and E. Viñuela.** 1985. Purification and properties of African swine fever virus. J. Virol. **54:**337–344.
8. **Carrascosa, J. L., J. M. Carazo, A. L. Carrascosa, N. García, A. Santisteban, and E. Viñuela.** 1984. General morphology and capsid fine structure of African swine fever virus particles. Virology **132:**160–172.
9. **Carrascosa, J. L., P. González, A. L. Carrascosa, B. García-Barreno, L. Enjuanes, and E. Viñuela.** 1986. Localization of structural proteins in African swine fever virus particles by immunoelectron microscopy. J. Virol. **58:**377–384.
10. **Costa, J. V.** 1990. African swine fever virus. p. 247–270. *In* G. Darai (ed.), Molecular biology of iridoviruses. Kluwer Academic Publishers, Boston, Mass.
11. **Dales, S., and E. H. Mossbach.** 1968. Vaccinia as a model for membrane biogenesis. Virology **35:**564–583.

12. **Dixon, L. K., D. Rock, and E. Viñuela.** 1995. African swine fever-like particles. Arch. Virol. Suppl. **10:**92–94.
13. **Dougherty, W. G., and B. L. Semler.** 1993. Expression of virus-encoded proteinases: functional and structural similarities with cellular enzymes. Microbiol. Rev. **57:**781–822.
14. **Enjuanes, L., A. L. Carrascosa, M. A. Moreno, and E. Viñuela.** 1976. Titration of African swine fever (ASF) virus. J. Gen. Virol. **32:**471–477.
15. **Esteves, A., M. I. Marques, and J. V. Costa.** 1986. Two-dimensional analysis of African swine fever virus proteins and proteins induced in infected cells. Virology **152:**192–206.
16. **González, A., A. Talavera, J. M. Almendral, and E. Viñuela.** 1986. Hairpin loop structure of African swine fever virus DNA. Nucleic Acids Res. **14:** 6835–6844.
17. **Grand, R. J. A.** 1989. Acylation of viral and eukaryotic proteins. Biochem. J. **258:**625–638.
18. **Griffiths, G., and P. Rottier.** 1992. Cell biology of viruses that assemble along the biosynthetic pathway. Semin. Cell Biol. **3:**367–381.
19. **Hellen, C. U. T., H. G. Kräusslich, and E. Wimmer.** 1989. Proteolytic processing of polyproteins in the replication of RNA viruses. Biochemistry **28:**9881–9890.
20. **Hellen, C. U. T., and E. Wimmer.** 1992. The role of proteolytic processing in the morphogenesis of virus particles. Experientia **48:**201–215.
21. **Hellen, C. U. T., and E. Wimmer.** 1992. Maturation of poliovirus capsid proteins. Virology **187:**391–397.
22. **López-Otín, C., J. M. P. Freije, F. Parra, E. Méndez, and E. Viñuela.** 1990. Mapping and sequence of the gene coding for protein p72, the major capsid protein of African swine fever virus. Virology **175:**477–484.
23. **Moura Nunes, J. F., J. D. Vigario, and A. M. Terrinha.** 1975. Ultrastructural study of African swine fever virus replication in cultures of swine bone marrow cells. Arch. Virol. **49:**59–66.
24. **Pettersson, R. F.** 1991. Protein localization and virus assembly at intracellular membranes. Curr. Top. Microbiol. Immunol. **170:**67–106.
25. **Puvion-Dutilleul, F., and E. Puvion.** 1995. Immunocytochemistry, autoradiography, in situ hybridization, selective stains: complementary tools for ultrastructural study of structure-function relationships in the nucleus. Applications to adenovirus-infected cells. Microsc. Res. Tech. **31:**22–43.
26. **Rome, L., A. J. Garvin, M. M. Allietta, and E. F. Neufeld.** 1979. Two species of lysosomal organelles in cultured human fibroblasts. Cell **17:**143–153.
27. **Roos, N., M. Cyrklaf, S. Cudmore, R. Blasco, J. Krinjse-Locker, and G. Griffiths.** 1996. A novel immunogold cryoelectron microscopic approach to investigate the structure of the intracellular and extracellular forms of vaccinia virus. EMBO J. **15:**2343–2355.
28. **Sanz, A., B. García-Barreno, M. L. Nogal, E. Viñuela, and L. Enjuanes.** 1985. Monoclonal antibodies specific for African swine fever virus proteins. J. Virol. **54:**199–206.
29. **Scheer, U., K. Messner, R. Hazan, I. Raska, P. Hansmann, H. Falk, E. Spiess, and W. W. Franke.** 1987. High sensitivity immunolocalization of double and single-stranded DNA by a monoclonal antibody. Eur. J. Cell Biol. **43:**358–371.
30. **Schloer, G. M.** 1985. Polypeptides and structure of African swine fever virus. Virus Res. **3:**295–310.
31. **Schweizer, A., J. Rohrer, J. W. Slot, H. J. Geuze, and S. Kornfeld.** 1995. Reassessment of the subcellular localization of p63. J. Cell Sci. **108:**2477–2485.
32. **Simón-Mateo, C., G. Andrés, F. Almazán, and E. Viñuela.** Unpublished data.
33. **Simón-Mateo, C., G. Andrés, and E. Viñuela.** 1993. Polyprotein processing in African swine fever virus: a novel gene expression strategy for a DNA virus. EMBO J. **12:**2977–2987.
34. **Sodeik, B., R. W. Doms, M. Ericsson, G. Hiller, C. E. Machamer, W. van't Hof, G. van Meer, B. Moss, and G. Griffiths.** 1993. Assembly of vaccinia virus: role of the intermediate compartment between the endoplasmic reticulum and the Golgi stacks. J. Cell Biol. **121:**521–541.
35. **Sogo, J. M., J. M. Almendral, A. Talavera, and E. Viñuela.** 1984. Terminal and internal inverted repetitions in African swine fever virus DNA. Virology **133:**271–275.
36. **Stephens, E. B., and R. W. Compans.** 1988. Assembly of animal viruses at cellular membranes. Annu. Rev. Microbiol. **42:**489–516.
37. **Towler, D. A., J. I. Gordon, S. P. Adams, and L. Glaser.** 1988. The biology and enzymology of eukaryotic protein acylation. Annu. Rev. Biochem. **57:** 69–99.
38. **Viñuela, E.** 1987. Molecular biology of African swine fever virus, p. 31–49. *In* Y. Becker (ed.), African swine fever. Nijhoff, Boston, Mass.
39. **Yáñez, R. J., J. M. Rodríguez, M. L. Nogal, L. Yuste, C. Enriquez, J. F. Rodríguez, and E. Viñuela.** 1995. Analysis of the complete nucleotide sequence of African swine fever virus. Virology **208:**249–278.